Exact Theory of Optical Transition Radiation in the Far and Near Zones

Ariel Nause,[1,*] Egor Dyunin,[2] Reuven Ianconescu,[2,3] and Avraham Gover[2]

[1] *Faculty of Exact Sciences, Department of Physics, Tel Aviv University, Israel*

[2] *Faculty of Engineering, Department of Physical Electronics, Tel Aviv University, Israel*

[3] *Shenkar College of Engineering and Design, Department of Electrical Engineering, Ramat Gan, Israel*

compiled: July 10, 2014

We present an exact solution of the complex field of Transition Radiation (TR) emitted by an electron incident on a conductive screen. The solution is valid in all space. In the reactive near zone it replicates the Coulomb fields of the electron and its image charge and their evolvement into radiation fields after termination of the charges current at the screen. Using a general formulation for radiation diffraction from a current line, we derive diffraction integral expressions in the reactive near-zone, the Fresnel near-zone and the Fraunhofer far-zone in analogy to diffraction from a planar radiation source. The derived exact complex field expressions can be useful for describing Coherent Optical TR (COTR) from a beam of phase-correlated charge particles in the near field and in the imaging plane of the screen.

1. Introduction

Transition radiation (TR) is the electromagnetic radiation emitted by a charged particle when it hits a conducting or dielectric plate or foil. The wide frequency band radiation emitted on both sides of a conductive foil originates from the Fourier components of the terminated (or correspondingly suddenly appearing) current of the charged particle in either side of the foil, as well as from the currents induced on the foil by the charge particle (see figure 1).

Transition radiation is a radiative emission process of basic interest on its own and as a possible practical source of radiation at a variety of different spectral regimes from THz radiation [1] to X-rays [2].

The first detailed theory of TR was published by Ginzburg and Frank [5]. They calculated the Coulomb transverse field component in the frequency domain of an electron of velocity v [6]:

$$\breve{E}_\rho(\rho,\omega) = \frac{e}{2\pi\epsilon_0}\frac{\omega}{c^2\gamma\beta^2}K_1\left(\frac{\omega}{\beta c\gamma}\rho\right) \tag{1}$$

$$\breve{H}_\phi(\rho,\omega) = \frac{e}{2\pi\epsilon_0}\frac{\omega}{c^2\gamma\beta}K_1\left(\frac{\omega}{\beta c\gamma}\rho\right) \tag{2}$$

where the Fourier transform is defined by $F\{f(t)\} = \int_{-\infty}^{\infty} f(t)\exp^{i\omega t}\,dt$, K_1 is the Bessel function of the first order, β is the particle velocity and γ is the Lorentz factor. In the relativistic limit these fields were assumed to be reflected from the screen like plane waves and diffracted towards an observation point in the far field.

Based on this model the *far field* energy per unit frequency per solid angle (spectral radiant intensity) emitted from a single charge hitting a perfect conductor at normal incidence is [2]:

$$\frac{dU_e}{d\Omega d\omega} = \frac{1}{4\pi\epsilon_0}\frac{e^2\beta^2}{\pi^2 c}\frac{\sin^2\theta}{(1-\beta^2\cos^2\theta)^2} \tag{3}$$

This expression has been used to calculate the TR emission energy distribution pattern in the far-field of a charged particle beam by convoluting it with the spatial and angular distribution function of the electron beam [3]. In the far field the spatial distribution of the e-beam does not affect the OTR radiation energy distribution from the e-beam [4]. However, when one considers OTR measurements in the near field diffraction zone (for example when one calculates the radiation distribution at the image plane of a camera viewing the OTR screen), Eq. (3) does not suffice.

Indeed expression (3) is not sufficient in neither the near or far field zones, if one needs to find the TR field emitted from a phase correlated electron beam (COTR) [7] [8]. In this case, an exact diffraction integral expression is required, including the radiation field phase. Shkvarunets and Fiorito [9] presented a more complete vector diffraction model based on Love's field equivalence theorem, but it was not employed for calculation of near field diffraction. Geloni et al developed related derivation of synchrotron and edge radiation near field analysis [10].

M. Castellano and V. Verzilov [11] described the fields of the unperturbed moving charge as a superposition

* Corresponding author: arielnau@post.tau.ac.il

of "pseudophotons" and calculated the OTR radiated field of a single electron as the superposition integral of those reflected pseudophotons. In this model (the Weizsäcker-Williams approximation) the pseudophotons are the spatial Fourier components of the K_1 fields of an unperturbed moving charge (Eqs. (1), (2)) that are proportional to the K_1 function, assuming that this is the field that is incident and reflected from the screen, from where free space diffraction starts. This model gives a good approximation for the complex field of the OTR radiation of ultra-relativistic charged particles in the near and far diffraction zones.

The Weizsäcker-Williams approximation model was used by Castellano and Verzilov [11] for calculating the spatial resolution of OTR imaging systems (used for beam diagnostics). The same model was used by Verzilov [12] to study the "pre-wave" zone of OTR radiation, namely the zone in the radiation emmision direction beyond the particle's incidence point. In this zone the Coulomb fields (Eqs. (1), (2)) that are bound to the electron trajectory within a transverse range $\beta\lambda\gamma$, transform into free diffraction radiation waves (this zone is termed in antenna theory and in the present article the "reactive near field zone").

Dobrovol'sky and Shul'ga considered the effect of finite size OTR target [14] and the interference effect of the diffracting OTR radiation waves and the Coulomb field of the propagating charge (in forward OTR) [13]. Both works used the conventional Weizsäcker-Williams model (based on the K_1 source approach) and considered only ultra-relativistic charges.

We present an exact vector field diffraction theory of TR from a single electron, based on dyadic Green function formulation [15]. The source of the diffraction integral is the current of the electron itself and its image charge. The complex field solution is exact at any distance: it reproduces on one hand the source Coulomb field of the electron at a proper distance before the electron hits the screen (1) (on the screen it produces a similar field only at relativistic energies) and on the other hand it exactly describes the radiation field in all optical diffraction regimes, including the "reactive near field", the Fresnel near field zone and the Fraunhofer far field. It can be then employed to calculate coherent and partially coherent TR radiation from temporally or spatial correlated electrons in an electron beam.

Optical Transition Radiation (OTR) is used extensively as diagnostics of the charge distribution across the cross-section of electron beams [16] and pulse duration [17]. In the application of OTR screens as e-beam profile diagnostics the screen is viewed by a camera focused to produce an image of the OTR screen on the camera sensor's screen. Assuming that there is no phase correlation between the radiation wave-packets emitted by the electrons which hit the OTR screen at different locations (namely the electrons hit the screen at random), the light density distribution on the camera image plane replicates the incident electron current distribution on the OTR screen. The e-beam profile image resolution is then limited only by the Modulation Transfer Function (MTF) of the camera. Thus in this application there is no need to know the coherent field (amplitude and phase) of the radiation wave-packets emitted by the individual electrons.

Recently coherence effects were observed in the measurement from OTR screens (COTR) [7]. The coherence effects came into expression as speckled images on the camera imaging plane and the integrated OTR power was not proportional to the e-beam current. The coherence effects that were described originally as "unexplained physics" [8] are now understood to be the results of correlation of the electrons arrival time due to a Coulomb collective micro-dynamic process in the e-beam transport line preceding the OTR screen [18]. Evidently, in order to interpret the imaged COTR radiation pattern at the camera sensors plane, one needs to know the coherent radiation field in the "near field diffraction zone" of the OTR screen and the Optical Transfer Function (OTF) of the camera optical system.

The radiation field on the screen is the result of coherent interference of the radiation fields of the electrons in the beam. Therefore, besides knowledge of the incidence phase of the electrons on the OTR screen, a necessary condition for composing the OTR screen coherent near field radiation pattern is an exact complex field expression of the OTR emission from an individual electron. The derivation of such an exact expression, valid in all near and far field regimes, is the goal of this paper. This formulation may be of interest priorly in connection to moderately relativistic and non relativistic protons and ions [19] and electrons [20].

The derivation of the exact TR diffraction equation in the article includes a general "line source" diffraction theory (as opposed to "surface source" in conventional diffraction theory). This formulation is generic an can be useful for various kinds of coherent line sources of radiation.

The paper is organized as follows: in Section 2 we define the formulation of the diffraction from a general line source. In Section 3 we identify the diffraction zones (near and far) of a line source in analogy to the Fresnel and Fraunhofer's diffraction zones from a surface source. In Section 4 we explain the formation zone and practical considerations for the integration range, and in Section 5 we implement the line source model to the case of TR and present computed results in different zones, including the "reactive near zone" (pre-wave zone).

2. Radiative Emission from a general line source

Diffraction theory has been developed primarily for analysis of radiation from a surface source. For the analysis of TR we need an electromagnetic diffraction theory from a line source. In the following two sections we present a general formulation for diffraction from a line current source of arbitrary axial distribution in the z

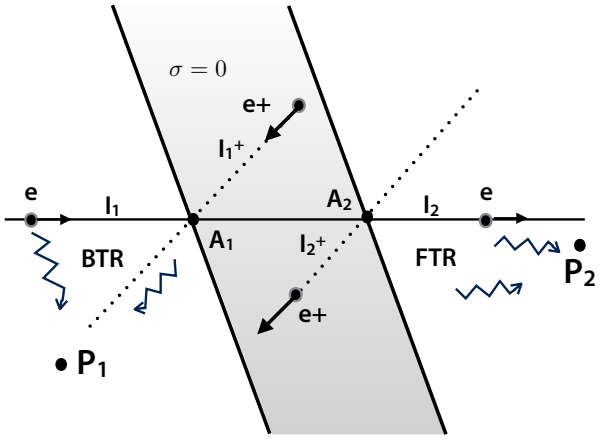

Fig. 1. The schemes of backward transition radiation (BTR) and forward transition radiation (FTR) for a perfect conductor foil screen and their equivalent image charge representation

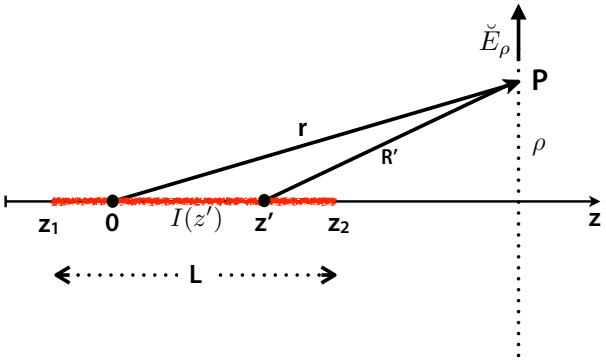

Fig. 2. Geometry of radiation diffraction from a current line source

direction:

$$\breve{\mathbf{J}}(\underline{r}',\omega) = \hat{\mathbf{e}}_z \breve{I}(z',\omega)\delta(x')\delta(y') \tag{4}$$

as shown in figure 2.

The electric field created by a current density $\breve{\mathbf{J}}(\mathbf{r})$ in frequency domain can be calculated as

$$\breve{\mathbf{E}} = -i\omega\mu \int G_e(\mathbf{r},\mathbf{r'})\breve{\mathbf{J}}(\mathbf{r'})\, d^3\mathbf{r'} \tag{5}$$

where $G_e(\mathbf{r},\mathbf{r'})$ is the Maxwell equation free-space dyadic Green function [15]:

$$G_e(\mathbf{r},\mathbf{r'}) = \left(\mathbf{I} + \frac{\nabla\nabla}{k^2}\right) \frac{e^{ik|\mathbf{r}-\mathbf{r'}|}}{4\pi|\mathbf{r}-\mathbf{r'}|} \tag{6}$$

where $\mathbf{r}$ and $\mathbf{r'} = \hat{\mathbf{e}}_z z'$ are the source and observation point coordinates, respectively (see figure 2). We employ equations (5) and (6) for a line source (4), and define $R' = \sqrt{\rho^2 + (z-z')^2}$, where ρ is the cylindrical coordinates radial component of the observation point P (see figure 2). The radiation field has transverse and axial components $\breve{\mathbf{E}} = \breve{E}_z\hat{\mathbf{e}}_z + \breve{E}_\rho\hat{\mathbf{e}}_\rho$. We are interested in the transverse electric field component. The radially symmetric field can then be expressed in terms of a longitudinal to transverse dyadic Green function element $G_\rho(\rho,z,z') = G_{\rho z}(\rho,z,z')$:

$$\breve{E}_\rho(\rho,z) = -i\omega\mu \int \breve{I}(z')G_\rho(\rho,z,z')\, dz' \tag{7}$$

where from (6) the longitudinal - transverse Green function is:

$$G_\rho = \frac{1}{k^2}\frac{\partial}{\partial\rho}\frac{\partial}{\partial z}\left(\frac{e^{ikR'}}{4\pi R'}\right) \tag{8}$$

or explicitly:

$$G_\rho = -\rho(z-z')\frac{e^{ikR'}}{4\pi R'^3}\left[1 + \frac{3i}{kR'} - \frac{3}{(kR')^2}\right] \tag{9}$$

The measurable optical parameter is usually the spectral power density. The expression for the spectral power density is derived from the Parseval theorem in the frequency range $0 < \omega < \infty$:

$$\int_{-\infty}^{\infty} \underline{S}(t) = \int_{-\infty}^{\infty} \underline{E}(t) \times \underline{H}(t) = \frac{1}{\pi}\int_0^{\infty} Re\left(\breve{\underline{E}}(\omega) \times \breve{\underline{H}}^*(\omega)\right) = \int_0^{\infty} \underline{S}(\omega)d\omega \tag{10}$$

For a line source (which has cylindrical symmetry), the axial spectral power density is:

$$S_z(\omega) = \frac{1}{\pi}\breve{E}_\rho(\omega)\breve{H}^*_\phi(\omega) \tag{11}$$

In the far-field only, in the paraxial approximation we may define the spectral radiant intensity as:

$$\frac{dU_e}{d\Omega d\omega} = \frac{z^2}{\pi}\sqrt{\frac{\epsilon_0}{\mu_0}}|\breve{E}_\rho(\omega)|^2 \tag{12}$$

where z is the coordinate of the observation plane relative to the source position.

3. The Diffraction Zones of a Line Source

Equations (7) and (9) constitute an exact diffraction integral formulation for a longitudinal current line source of any current distribution. As in diffraction theory from a planar source, it is possible to define also for a line source approximate diffraction integrals and diffraction zones analogous to the reactive near-field zone, the Fresnel diffraction near-field zone and the Fraunhofer diffraction far-field zone of a planar source.

In most practical cases we are interested in the field

in a spatial range longer than a wavelength:

$$kr = 2\pi r/\lambda \gg 1 \tag{13}$$

In this range the Green function (9) can be replaced by:

$$G_\rho = -\rho(z-z')\frac{e^{ikR}}{4\pi R^3} \tag{14}$$

In the diffraction zones, we can further approximate (14) by employing series expansion of R in terms of $\frac{z'}{r}$ where (see figure 2):

$$R' = [(z-z')^2+\rho^2]^{\frac{1}{2}} = [(z^2-2zz'+z'^2+\rho^2]^{\frac{1}{2}} = r[1-2\frac{zz'}{r^2}+\frac{z'^2}{r^2}]^{\frac{1}{2}} \tag{15}$$

where we defined $r=\sqrt{(z^2+\rho^2)}$ - the distance of the observation point from the coordinates origin. The expansion in terms of $\frac{z'}{r}$ is analogous to the expansion in terms of the source transverse coordinates in the case of diffraction from a planar source.

3.A. Longitudinal Quadratic-Phase "Fresnel" Near Zone Limit

Defining $\cos\theta = \frac{z}{r}$, second order Taylor expansion results in:

$$R' \simeq r[1-\frac{z'}{r}\cos\theta+\frac{1}{2}\frac{z'^2}{r^2}\sin^2\theta] \tag{16}$$

This result is now substituted into the Green function phase (14). In the denominator we substitute only the zero order $R' \simeq r$. This results in the longitudinal-to-transverse Green function expression in a quadratic-phase paraxial approximation zone (analogous to the convention of Fresnel zone in the case of a transverse current source):

$$G_\rho = -\sin\theta\cos\theta\frac{e^{ikr}}{4\pi r}e^{-ik_z z'+ik\sin^2\theta\frac{z'^2}{2r}} \tag{17}$$

where $k_z = k\cos\theta$.

Substituting (17) in (7), the "Fresnel" integral of an axial line current source is:

$$\breve{E}_\rho = \frac{i\omega\mu}{4\pi}\frac{e^{ikr}}{r^3}\rho\int_{z_1}^{z_2}\breve{I}(z')e^{-ik(\cos\theta z'+\sin^2\theta\frac{z'^2}{2r})}(z-z')dz' \tag{18}$$

for a general sinusoidal current distribution $\breve{I}(z)\propto e^{ik_0 z}$ this integral can be expressed in terms of the traditional Fresnel integrals $c(x)=\int_0^x\cos(t^2)dt$, $s(x)=\int_0^x\sin(t^2)dt$.

The validity range of the "Fresnel" quadratic phase approximation is determined by the requirement that the contribution of the third order expansion of (14) to the Green function phase is much smaller than π and is neglected. When also the quadratic phase term in (18) is much smaller than π, it can also be dropped, and then the "Fresnel" near field approximation turns into the "Fraunhofer" far field approximation, that is considered in the next section.

Using $|z'|<L$, the "Fresnel" near field diffraction zone of the longitudinal line current is defined in the range:

$$\left(\frac{L^3\rho^2 z}{8\pi\lambda}\right)^{1/5} \ll r \ll \left(\frac{\rho^2L^2}{\lambda}\right)^{1/3} \tag{19}$$

where L is the length of the radiation line-source.

Note that in the derivation of (17) and (18) we did not need to resort to the paraxial approximation $\rho \ll z$. In the paraxial approximation $r\approx z$ and the LHS of (19) is replaced by

$$\left(\frac{L^3\rho^2}{8\pi\lambda}\right)^{1/4} \ll z \tag{20}$$

Also note that in the near diffraction zone, contrary to the far zone, the parameters r, $\sin\theta=\rho/r$, $\cos\theta=z/r$ are not uniquely defined, and depend on the choice of origin $z'=0$ of the line source function (see figure 2). Therefore, the radiation pattern $\breve{E}_\rho(\omega,z,\rho)$ may seem somewhat different for different choice of origin.

3.B. Longitudinal "Fraunhofer" Far Zone Limit

In the Fraunhofer diffraction far zone limit, the quadratic term of the phase is negligible. In analogy to the planar source case, the far zone of a line source is defined by the requirement that the quadratic phase term in the exponent of (17) is negligible, resulting:

$$z \cong r \gg \left(\frac{\rho^2L^2}{\lambda}\right)^{1/3} \tag{21}$$

The longitudinal-to-transverse Green function in the Fraunhofer limit is then:

$$G_\rho = -\sin\theta\cos\theta\frac{e^{ikr}}{4\pi r}e^{-ik_z z'} \tag{22}$$

The line source far-field diffraction integral is then:

$$\breve{E}_\rho = \frac{i\omega\mu}{4\pi}\frac{e^{ikr}}{r}\sin\theta\cos\theta\int_{z_1}^{z_2}\breve{I}(z')e^{-ik_z z'}dz' \tag{23}$$

4. Ginzburg's Formation Zone

The derivation so far is general for any longitudinal current line-source. We now specify to the case of OTR emission from an electron incident on a conducting screen.

Radiation from a free electron is always formed in a finite region and not in a point. This region is considered the "formation zone" according to Ginzburg [21]. The formation zone size is dependent on the emission wavelength λ. Its size is termed the "formation length"- L_f. The formation length is essentially the length of

traversal in free space of a charged particle, such that the radiation emitted by it at wavelength λ accumulates at the observation point a phase increment of 2π.

Ginzburg's formation length is [21]:

$$L_f = (1+\beta)\gamma^2\lambda \approx 2\gamma^2\lambda \tag{24}$$

The second part of the equation is for $\beta \simeq 1$.

The diffraction formula integration (7), employed in the case of TR to the charged particle current, is supposed to be carried out in the ideal case from $-\infty$ to 0 or from 0 to ∞. In practice, the radiation emission from the electrons well before the formation zone ($L > L_f$) is negligible. This consideration provides a practical range for performing the numerical integration of the diffraction integral. We will investigate this consideration using the exact solution for different lengths in units of the formation length in order to verify the convergence of our solution.

5. Transition Radiation Model

Let us consider now the case of transition radiation emission from a perfect conductor foil screen set at arbitrary angle relative to the electron propagation direction as shown in figure 1. An observer at P_1 in the half space before the foil would sense the non radiative Coulomb fields of the electron (both electric and magnetic - due to the electron velocity [6]) only if it is positioned very close (distance $\sim \beta\gamma\lambda/2\pi$) to the electron trajectory. This field is the same as the Coulomb field of an unperturbed moving charge (Eqs. (1), (2)), if observed far enough before the screen. However, because the electron charge vanishes upon incidence on the screen, as it seems in the back half space, the abrupt temporal change in the electron current I_1 means that its Fourier spectrum contains a very wide band of frequencies, and these current spectral components radiate in free space, and would be sensed by observer P_1 at any finite distance away from the screen.

The radiation from the terminated current I_1 is not the only source of BTR radiation. The other, more dominant contribution to BTR radiation is the surface current on the screen due to the time varying positive surface charge induced on the conductor screen by the approaching negatively charged electron, which vanishes almost instantaneously (at the dielectric relaxation time of the conductor) when the electron is incident on the screen. Also these time varying surface currents radiate in a wide frequency band, and their radiation would be sensed at point P_1 as well.

Using the method of equivalent charge images [15], we assert that the induced current on the infinite conductor screen radiates into the half space exactly like an imaginary point particle of charge $+e$ that propagates along the trajectory of the mirror image (relative to the screen surface) of the electron e, and is represented by current I_1^+ in figure 1. This current terminates exactly at the same time of the electron's incidence on the screen. The combined radiation fields from both sources is the Backward Transition Radiation (BTR).

A similar physical process takes place in the forward half space of the screen, if it is made of a thin foil, through which the electron emerges into the forward half space abruptly. The Forward Transition Radiation (FTR) observed at point P_2 in this half space is the same as generated in an equivalent picture of electron current I_2 and a positive image charge current I_2^+, both appear to be generated abruptly in time in the forward half space (see figure 1).

Taking the charge propagation direction to be along coordinate z, and arbitrarily choosing the coordinate origin $z = 0$ at the particle intersection point with the conductor surface (A_1 or A_2), the current densities corresponding to currents I_1, I_1^+, I_2, I_2^+ are:

$$\mathbf{J}_1(\mathbf{r},t) = -e\delta(x-x_0)\delta(y-y_0)\delta[z-v(t-t_0)][1-\eta(t-t_0)] \tag{25}$$
$$\mathbf{J}_1^+(\mathbf{r},t) = +e\delta(x-x_0)\delta(y-y_0)\delta[z-v(t-t_0)][1-\eta(t-t_0)] \tag{26}$$
$$\mathbf{J}_2(\mathbf{r},t) = -e\delta(x-x_0)\delta(y-y_0)\delta[z-v(t-t_0)]\eta(t-t_0) \tag{27}$$
$$\mathbf{J}_2^+(\mathbf{r},t) = +e\delta(x-x_0)\delta(y-y_0)\delta[z-v(t-t_0)]\eta(t-t_0) \tag{28}$$

where (x_0, y_0) and t_0 are respectively the coordinates and time of incidence (or emergence) of the real or imaginary charge particle at the screen. The η function is defined as:

$$\eta(t-t_0) = \left\{ \begin{array}{ll} 1 & t > t_0 \\ 0 & t < t_0 \end{array} \right\} \tag{29}$$

Fourier transforming over time and integrating over transverse coordinates, the corresponding spectral currents are:

$$\breve{I}_1(z) = -ee^{i\omega t_0}e^{i\frac{\omega}{v}z}[1-\eta(z)]\eta(z+L) \tag{30}$$
$$\breve{I}_1^+(z) = +ee^{i\omega t_0}e^{i\frac{\omega}{v}z}[1-\eta(z)]\eta(z+L) \tag{31}$$
$$\breve{I}_2(z) = -ee^{i\omega t_0}e^{i\frac{\omega}{v}z}[1-\eta(z-L)]\eta(z) \tag{32}$$
$$\breve{I}_2^+(z) = +ee^{i\omega t_0}e^{i\frac{\omega}{v}z}[1-\eta(z-L)]\eta(z) \tag{33}$$

Here we included a finite electron trajectory length L before or after the screen to account for injection or termination of the electron beam. Since most of the TR is generated in the Ginzburg formation length [21], the diffraction integrals should be independent on L only if:

$$L \gg L_f \tag{34}$$

in which case one may set $L = \infty$. However, it is desirable to keep L finite, not only for purposes of numerical computation, but because in practical situations (high electron beam energy, finite screen dimensions) the effective interaction length L is realistically finite.

In principle, the diffraction fields of both $\breve{I}_1$ and $\breve{I}_1^+$ (for BTR) need to be calculated separately and summed up coherently and vectorially at the observation point P_1 (and correspondingly so with $\breve{I}_2$ and $\breve{I}_2^+$ for FTR). This is essential when the electron is not relativistic and its radiation lobe has wide angle [22], [20]. In these cases one must consider the fields generated by both currents and sum up coherently their amplitudes that interfere in the observation point P_1. In the present work we neglect this effect and consider the more common case of a relativistic charged particle beam. In this case, the radiation lobes of I_1^+ (for BTR) and I_2 (for FTR) are Doppler frequency up-shifted and their angular width is narrow ($2/\gamma \ll \pi/2$). The radiation lobes of the other current components are Doppler down-shifted and their interference with the main lobes may be neglected.

In the following we analyze the exact and approximate diffraction integrals of I_1^+, which is the relevant current source for the more useful BTR measurement scheme. The conclusions we derive are equally valid for the other current sources.

5.A. Exact Solution

We substitute $I_1^+(z)$ (31) as the line current source in the diffraction integral (7) with the exact Green function (9).

$$\breve{E}_\rho = -\frac{i\omega\mu e}{4\pi} e^{i\omega t_0} \int_{-L}^{0} \frac{\rho(z-z')}{R'^3}\left(1 + \frac{3i}{kR'} - \frac{3i}{(kR')^2}\right)\times e^{ik\left(R' + \frac{z'}{\beta}\right)}\, dz' \tag{35}$$

If the observation point position satisfies $kR' \gg 1$ (a sufficient condition is that it is more than a wavelength off axis anf off the screen), then a good approximation for (35) is:

$$\breve{E}_\rho = -\frac{i\omega\mu e}{4\pi} e^{i\omega t_0} \int_{-L}^{0} \frac{\rho(z-z')}{R'^3} e^{ik\left(R' + \frac{z'}{\beta}\right)}\, dz' \tag{36}$$

Here $z' = -L$ is the inception point of the drifting electron and $z' = 0$ is its termination point on the screen.

It is important to note that OTR is not emitted instantaneously at the incidence of the electron on the screen, but during its entire traversal time from the point of inception up to the screen incidence time. As discussed in section 4, most of the contribution to the TR field is accumulated during the electron traversal through Ginzburg's formation zone $-L_f < z < 0$. In figure 3 we examine numerically for a specific example convergence of the transverse distribution of the OTR field amplitude squared to a finite value as L is increased to the limit $L \gg L_f$. Equation (36) was integrated for exemplary parameters: $\beta = 0.9999$ ($\gamma = 75$), $\lambda = 1\mu m$ ($L_f = 11mm$) and observation plane in the far field zone at $z = 10m$. The absolute value squared of the OTR field $|\breve{E}_\rho|^2$ is shown in figure 3 as a function of the transverse coordinate ρ for different values of L. It is seen that the curves converge slowly to a stable value as L increases. In this particular example $N = L/L_f > 1$ provides convergence within 5% to the analytical solution of a semi-infinite long beam (see equation (39) in the next section).

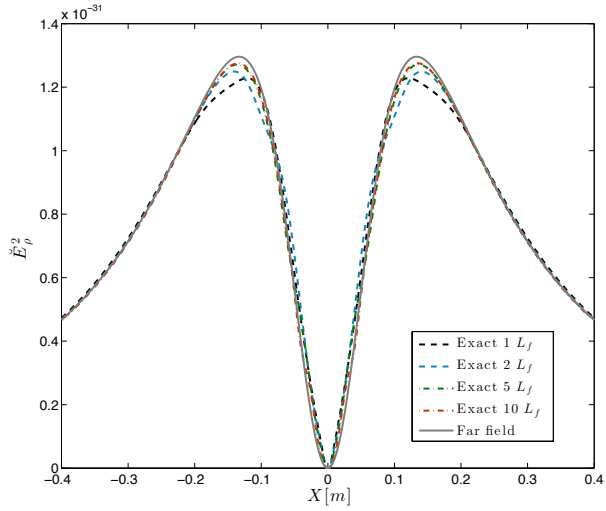

Fig. 3. Transverse electric field amplitude squared of TR in the far field zone ($\lambda = 1\mu m$, $\gamma = 75$ at a distance of $10m$). Different curves are for increasing integration lengths in formation length units

5.B. Far Field Approximation

Using the longitudinal Fraunhofer approximation of section 3.B, we substitute the Fraunhofer Green function (22) and the image-charge current source $I_1^+(z)$ (31) in equation (7), and obtain for the case of BTR:

$$\breve{E}_\rho = -\frac{\omega\mu e}{4\pi r} e^{i\omega t_0} \frac{1}{\left(\frac{\omega}{v} - k_z\right)} \sin\theta\cos\theta \tag{37}$$

Substituting $k_z = \frac{\omega}{c}\cos\theta$, we find the far-field approximation for the electric field:

$$\breve{E}_\rho = -\frac{\mu ce}{4\pi r} e^{i\omega t_0} \frac{1}{\frac{1}{\beta} - \cos\theta} \sin\theta\cos\theta \tag{38}$$

Taking the square of the absolute value,we get for small angles:

$$|\breve{E}_\rho|^2 = \frac{\mu^2 c^2 e^2 \beta^2}{16\pi^2 z^2} \frac{\sin^2\theta}{(1-\beta\cos\theta)^2} \tag{39}$$

Finally, using (12) and $c^2 = 1/\mu_0\epsilon_0$ we obtain the well-known result for the far-field TR pattern:

$$\frac{dU_e^2}{d\Omega d\omega} = \frac{e^2\beta^2}{16\pi^3}\sqrt{\frac{\mu_0}{\epsilon_0}} \frac{\sin^2\theta}{(1-\beta\cos\theta)^2} \tag{40}$$

that is identical with (3) in the limit $\beta \simeq 1$.

The analytical expression (39) for a semi infinite electron trajectory is presented in figure 3 in a solid line, shown to be the limit of convergence of the numerical solution in the far field zone and $L \to \infty$.

As indicated earlier, the complete TR field should include (for BTR) also the contribution of the real electron current $\breve{I}_1(z)$ (30) summed up coherently and vectorially with the main field contribution of the image charge (38). This contribution turns out to be

$$\breve{E}_\rho = \frac{\mu ce}{4\pi r} e^{i\omega t_0} \frac{1}{\frac{1}{\beta} + \cos\theta} \sin\theta\cos\theta \tag{41}$$

In the case of normal incidence on the screen (and only in this case) the total BTR field is given as the algebraic sum of (38) and (41), resulting in the more complete expression (3) for the total BTR spectral radiant intensity in the far diffraction zone. In the ultra-relativistic regime the radiation lobe of the image charge (38) becomes narrow and intense in the direction of I_1^+ while the radiation lobe of the real charge (41) remains wide and negligible relative to that of the image charge. In this case (40) and (3) are identical.

5.C. Fresnel Approximation

In the longitudinal quadratic phase ("Fresnel") approximation (section 3.A), the transverse electric field is given by equation (18). We apply the diffraction formula, integrating over $I_1^+(z)$ (31).

Figure 4 presents the results of the numerical computation for the distance of $z = 10cm$ ($\gamma = 75$), which is well within the approximation regime (19). We display the results of the computation with the exact diffraction formula (35) and with the "Fresnel" diffraction formula (18). The curves overlap. The integration length used was one formation length. We also display for comparison the field radiation pattern that would be expected from the far-field formula (39).

The example shows good match between the exact and the Fresnel solutions, while the far field approximation curve differs significantly, both in amplitude and peak locations.

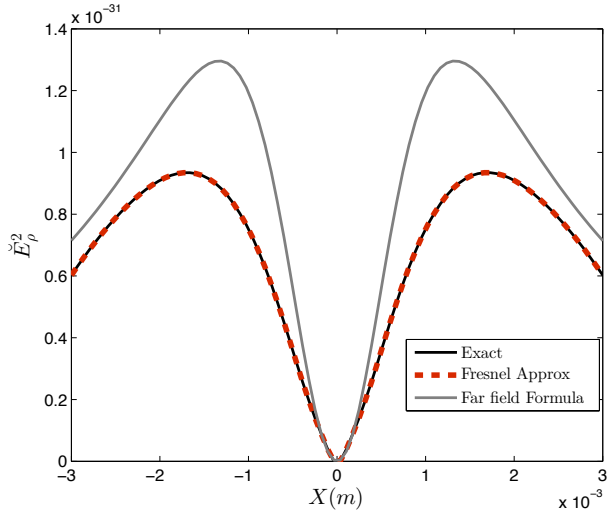

Fig. 4. Transverse electric field amplitude in the near field zone of TR ($\lambda = 1\mu m$, $\gamma = 75$, $z = 10cm$). The exact solution and the Fresnel approximation, computation results overlap. The numerical integration was performed over 1 formation length. We show for comparison the field radiation pattern that would be predicted from the far zone formula (39).

5.D. Reactive near field regime

It is evident that there is a spatial range in which the Coulomb fields that are attached to the electron (or its image charge) detach from the charged particle and transform into free space diffracting radiation waves. This range, analogous to the reactive near zone in antenna theory, was investigated by Verzilov in [12] using the Weizsäcker-Williams approximation. In this zone, also called the "pre-wave" zone the optical diffraction theory (including the Fresnel near field diffraction formulae) does not apply. The wave zone range can be determined from (20) for a general line source, where for the case of TR from a relativistic beam we set $\rho/z = \gamma$ and an effective line source length of $L = L_f$ (Eq. (24)). The inverse inequality defining the "pre-wave zone" is as in [12]:

$$z \ll L_f \tag{42}$$

Our exact TR formula (35) is valid in all space, including the "pre-wave zone" (42) and the Coulomb fields range $z < 0$ (relevant only for the field of $\breve{I}_1(z)$). It is instructive to test this validity by comparing the computed field in these zones to the Coulomb field (1) of an unperturbed drifting electron (propagating from $-\infty$ to ∞). At the same time we probe the validity of the Weizsäcker-Williams approximation that underlies the previously used models.

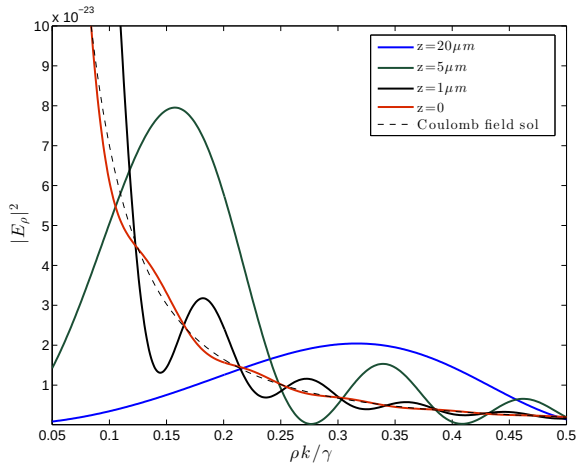

Fig. 5. Transverse electric field amplitude calculated using the exact solution at various observation distances in the reactive near-field compared to the Coulomb field of a relativistic particle (1). This demonstrates the transition of the Coulomb field to radiation field. X-axis values are presented in normalised units $\rho k/\gamma$.

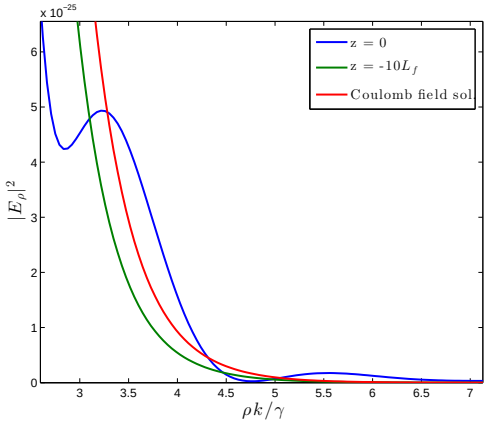

Fig. 6. Comparison of the exact solution with the Coulomb field solution for a moderate relativistic case of $\gamma = 2.95$. The integration is over a range of $40L_f$, where $L_f = 17.4\mu m$. The exact solution at $z = -10L_f$ resembles to the Coulomb field solution, but the difference between the incident field, i.e. the exact solution at $z = 0$ and the Coulomb field solution is evident. X-axis values are presented in normalised units $\rho k/\gamma$.

Figure 5 presents the transverse electric field variation as a function of ρ calculated for an example of ultra-relativistic beam ($\gamma = 75$), using the exact solution (35) in the reactive near-field zone - $z = 0, 1, 5, 20\mu m$. The Bessel K_1 function solution of the analytical Coulomb field expression [6] in the frequency domain is also shown for comparison (broken line), validating for this example the assumption of the Weizsäcker-Williams approximation model, namely that the electric field incident on the screen at $z = 0$ is almost the same as the field of an unperturbed drifting electron (1). The horizontal coordinate is presented in normalised units $\rho k/\gamma$. The reconstruction of the Coulomb field is very good. The figure demonstrates vividly the transition of the electron Coulomb field to radiation field in the near field ("pre-wave") zone.

We showed here that for an ultra-relativistic beam the computed field distribution emitted by I_1^+ right after the point of incidence on the screen ($z = 0$) is similar to the Coulomb field of an unperturbed drifting electron (K_1 distribution), which is the assumption of the commonly used Weizsäcker-Williams approximation. This is not the case for a non relativistic or even a moderately relativistic beam. This observation and the realization that the radiation source is a line source, rather than a planar source, may have implication on the focusing condition of the lens when imaging OTR and would affect the image resolution.

5.E. Non relativistic and moderately relativistic case

As mentioned before the conventional K_1 model is a good approximation for the ultra-relativistic case, but the method developed in this work is accurate for any velocity of the charges. The example shown in Figure 6 corresponds to a moderately relativistic beam ($\gamma = 2.95$). It demonstrates the difference between the fiels distribution of the incoming electron (I_1^+) before incidence on the screen ($z \leq 0$) obtained with the current formalism and the K_1 approximation for the case of moderately relativistic beam. From Figure 6 it is clear that the field incident on the screen ($z = 0$) is different from the K_1 approximation. The transverse range over which the exact solution differs from the K_1 approximation is of the order of a wavelength λ and therefore it

would not affect significantly the far field radiation pattern. The difference would be more significant for a non relativistic beam example, in which case the Weizsäcker-Williams model assumptions are not valid.

For comparison, Figure 6 displays the computed Coulomb field distribution of the incoming electron also in a plane $z = -10L_f$, far enough before the screen. In this case, the computed solution looks similar to the K_1 curve (Eq.(1)) in the coordinates scale shown.

6. Conclusions

We present in this paper an exact formulation for computing the transition radiation complex field of an electron incident on a perfect conductor screen at any angle. The derivation is based on a general dyadic Green function solution of the field radiation from a line current source of arbitrary distribution. The general line source solution yields approximate diffraction integral expressions in the reactive near-field zone, the quadratic phase "Fresnel" zone and the "Fraunhofer" far-field zone. Applying the general formulation to the case of transition radiation we obtained new TR diffraction integral expressions in all diffraction zones. The computation results replicate the standard TR radiation formula in the far field when the electron path is semi-infinite. It also demonstrates vividly the transition of the electron Coulomb field into radiation field after the incidence point and it shows that the field incident on the screen differs from the K_1 approximation.

The result of exact complex field solution from a single electron, including both amplitude and phase, would be useful for simulating imaging of coherent OTR effects, which are the result of coherent interference of the radiation field from an electron beam in which the electron distribution is phase correlated. In addition, the formalism presented in this work allows OTR calculations from beams in which the charges do not necessarily have a constant velocity.

In conclusion, we point out that even though the formulation derived in this paper referred to electrons, it applies as well (except for a change of sign of the field for positive charge) to any charged particle beam as protons or ion beams. In fact, the derivation may be more relevant for these cases, that are often in the non relativistic or moderately relativistic regime.

7. Acknowledgement

this research was supported by a grant from the United States-Israel Binational Science Foundation (BSF), Jerusalem, Israel.

References

[1] N.A. Vinokurov. "The generator of high-power short thz pulses." In *Proceedings of FEL2012, Nara, Japan*, 2012.

[2] M. Ter Mikaelian. "High Energy Electromagnetic Processes in Condensed Media." *Wiley*, 1975.

[3] G. L. Orlandi "Coherence effects in the transition radiation spectrum and practical consequences" *Optics Communications*, 211:109–119, 2002.

[4] E. Chiadroni, M. Castellano, A. Cianchi, K. Honkavaara, and G. Kube "Effects of transverse electron beam size on transition radiation angular distribution" *Nuclear Instruments and Methods in Physics Research A*, 673:56–63, 2012

[5] V.L. Ginzburg I.M. Frank. "Transition radiation." *Zh. Eksp. Teor. Fiz.* 16(1):15–22, 1946.

[6] C. A. Brau. "Modern Problems in Classical Electrodynamics." *Oxford* University Press, New York, 2004.

[7] A. H. Lumpkin. "First observations of COTR due to a microbunched beam in the VUV at 157mm." *Nuclear Instruments and Methods in Physics Research A*, 528:194–198, 2004.

[8] R. Akre et al. "Commissioning the linac coherent light source injector." *Phys. Rev. ST Accel. Beams*, 11:030703, 2008.

[9] A. G. Shkvarunets and R. B. Fiorito. "Vector electromagnetic theory of transition and diffraction radiation with application to the measurement of longitudinal bunch size." *Physical Review Special Topics*, 11(012801), 2008.

[10] G. Geloni, E. Saldin, E. Schneidmiller, and M. Yurkov. "Fourier treatment of near-field synchrotron radiation theory." *Optics Communications*, 276(1):167 – 179, 2007.

[11] M. Castellano and V. A. Verzilov "Spatial resolution in optical transition radiation beam diagnostics" *Physical Review Special Topics Accelerators and Beams*, 1:062801 , 1998.

[12] V. A. Verzilov "Transition radiation in the pre-wave zone" *Physics Letters A*, 273:135 – 140 , 2000.

[13] N.F. Shul'ga and S.N. Dobrovol'sky "About transition radiation by relativistic electrons in a thin target in the millimeter range of waves" *Physics Letters A*, 259:291 – 294 , 1999.

[14] S.N. Dobrovol'sky and N.F. Shul'ga "Transversal spatial distribution of transition radiation by relativistic electron in the formation zone by the dotted detector." *Nuclear Instruments and Methods in Physics Research B*, 201:123 – 132 , 2003.

[15] R. E. Collin. "Field Theory of Guided Waves." *IEEE Press Series on Electromagnetic Wave Theory*, 1990.

[16] G. Geloni, P. Ilinski, E. Saldin, E. Schneidmiller, and M. Yurkov. "Method for the determination of the three-dimensional structure of ultrashort relativistic electron bunches." *Deutsches Elektronen-Synchrotron* DESY, Hamburg, May 2009.

[17] E. Schneidmiller E. Saldin and M. Yurkov. "A simple method for the determination of the structure of ultrashort relativistic electron bunches." *Nucl. Instrum. Meth. A*, 539:499, 2005.

[18] A. Gover and E. Dyunin. "Collective-interaction control and reduction of optical frequency shot noise in charged-particle beams." *Phys. Rev. Lett.*, 102(15):154801, Apr 2009.

[19] R.B. Fiorito, D. Feldman, A.G. Shkvarunets "Final report on optics and candidate optical emissions for imaging the ORNL SNS target" *Institute for Research in Electronics and Applied Physics, University of Maryland, College Park, MD 20742*, February 27, 2008.

[20] R.B. Fiorito, D. Feldman, A.G. Shkvarunets, S. Casey, B.L. Beaudoin, B. Quinn, P.G. O'Shea "OTR measurements of the 10 kev electron beam at the University of Maryland electron ring (UMER)" In *Proceedings of*

PAC07, Albuquerque, New Mexico, USA, June 25-29, 2007.

[21] V.L. Ginzburg. "Transition radiation and transition scattering." *Physica Scripta Volume T*, 2:182–+, June 1982.

[22] L. Wartski. "Interference phenomenon in OTR and its application to particle beam diagnostics and multiple scattering measurements." *J. Appl. Phys.*, 48(3646), 1975.